Mechanisms of carbon dioxide detection in the earthworm *Dendrobaena veneta*.

E Jordan Smith[1,2], Jennifer L Ryan[1], Sofia A Lopresti[1], Dastan BS Haghnazari[1], Karleigh AS Anderson[1], Sarah J Lipson[1], Erik C Johnson[1], Wayne L Silver[1], Cecil J Saunders [1,3]

1 Department of Biology, Wake Forest University, Winston-Salem, NC, 27106, USA

2 Department of Biology, Boston University, Boston, MA, 02215, USA

3 Department of Biological Sciences, Kean University, Union, NJ, 07083, USA

Author contributions:

First authorship – ES
Senior authorship – CS

Corresponding author(s): CS csaunder@kean.edu, jakesaunders@gmail.com; ES smithej@bu.edu, emi.jor.smi@gmail.com

ES, KA, EJ, WS, and CS contributed to the conception and design of the study. ES developed the exudate assay and with JR, SL, and DH, conducted experiments with that assay. KA and CS optimized the RNA extraction protocol. KA, SL, and CJS organized and analyzed transcriptomic data. ES wrote the first draft of the manuscript with major input from CJS. All authors read and approved the submitted version.

Abstract
Carbon dioxide (CO_2) is a critical biological signal that is noxious to many animals at high concentrations. The earthworm *Dendrobaena veneta* lives in subterranean burrows containing high levels of CO_2 and respires through its skin. Despite the ecological and agricultural importance of earthworms, relatively little is known about how they make decisions in their environment, including their response to elevated levels of CO_2. To examine CO_2 detection in this species, we designed the exudate assay, in which we placed an earthworm in a sealed container, exposed it to varying concentrations of CO_2 for one minute, and recorded the amount of exudate secreted. Because earthworms excrete exudate in response to noxious stimuli, we hypothesized that the amount of exudate produced was proportional to the amount of irritation. We repeated these experiments after treatment with several blockers for molecules with potential involvement in CO_2 detection, including carbonic anhydrases, guanylate cyclase, TRPA1 channels, ASICs, and OTOP channels. We also confirmed the presence of homologous transcripts for each of these gene families in an epithelial transcriptome for *D. veneta*. Additionally, since organisms often detect CO_2 levels indirectly by monitoring the conversion to carbonic acid (a weak acid), we used the exudate assay to evaluate aversion to additional weak acids (formic acid, acetic acid, and propionic acid). Earthworms excreted significantly more exudate in response to CO_2 in a dosage-dependent manner, and this response was muted by the general carbonic anhydrase inhibitor acetazolamide, the carbonic anhydrase IX/XII inhibitor indisulam, the calcium channel blocker ruthenium red, the sodium channel blocker amiloride, and the acid-sensing ion channel blocker diminazene aceturate. These data provide evidence of the role of carbonic anhydrase and ENaCs in earthworm CO_2 detection and contribute to our understanding of the mechanisms used by earthworms to detect and react to weak acids in their environment.

Keywords:
Eisenia hortensis
European nightcrawler
carbonic anhydrases
chemical senses
chemosensory
epithelial sodium channels
degenerin
TRPA1

Contribution to the field statement:
Carbon dioxide (CO_2) is a major byproduct of cellular respiration and an important biological signal. The metabolism of animals living underground in burrows can cause the concentration of CO_2 to increase above atmospheric CO_2. Most animals have multiple molecular mechanisms that detect CO_2 and find high concentrations aversive or noxious; some subterranean animals have adaptations that make them more tolerant of concentrated CO_2. Earthworms live in burrows, are a keystone species for subterranean ecosystems, and in their lightless environment must rely primarily on tactile and chemical signals. Despite the profound importance of earthworms to the ecosystems, few if any of the molecular mechanisms they use to detect these signals have been characterized. Here we use RNA sequencing to develop a list of candidate mechanisms that the European nightcrawler may use to respond to CO_2. We also have developed an assay for comparing how noxious different concentrations of volatile compounds are to earthworms. In the present study, we utilize that assay with inhibitors to further narrow the possible multiple molecular mechanisms responsible for the detection of CO_2. We suspect that our study is among the first attempts to combine RNA-sequencing technology and pharmacology to describe earthworm sensory biology.

Introduction

As a major byproduct of cellular respiration, CO_2 is pervasive in most ecosystems and may indicate the presence of other living organisms. It is thus a critical signaling molecule that is often attractive or aversive depending on the organism and concentration. Fruit flies, for example, avoid CO_2 released by neighboring stressed flies (Suh et al., 2004), while mosquitoes are attracted to CO_2 emitted by their hosts (Spanoudis et al., 2020). At higher concentrations, CO_2 can be noxious, and may result in hypercapnia, hypoxia, or anesthesia (Cummins et al., 2019). Given its biological prevalence, potential health risks, and environmental relevance, it is critical to understand the mechanisms by which organisms detect CO_2.

Important decomposers in some ecosystems and invasive species in others, earthworms play critical roles in environmental health and agriculture. In many ecosystems, earthworms are

a key component of soil fertility, influencing soil turnover, soil aeration, and nutrient availability (Edwards, 2004). Despite their essential environmental role, we know little about what chemicals attract and repel earthworms nor the mechanisms by which they detect those chemicals (Silver et al., 2019; Reed et al., 2021). One such chemical is carbon dioxide (CO_2). The current concentration of CO_2 in air is approximately 0.04% (Amundson & Davidson, 1990; Scott, 2011). Earthworms live in burrows up to three meters deep and may encounter CO_2 concentrations of .04% to 13.0% (Amundson & Davidson, 1990). Some subterranean organisms, such as naked mole rats, have unique adaptations that allow them to tolerate normally noxious concentrations of CO_2 (Shams et al., 2005; Fang et al., 2014); earthworms may have similar adaptations.

The ubiquitous presence and broad importance of CO_2 has produced multiple detection pathways across organisms (Figure 1A). Most mechanisms require carbonic anhydrase, which catalyzes the reversible conversion of carbon dioxide into a bicarbonate ion and a proton, reacting with water from extracellular fluid (Lindskog, 1997). Carbonic anhydrase is found across animals, plants, and microorganisms, includes three independently evolved isozyme families, and is essential in many biological functions including metabolism, cellular transport, and acid-base balance (Henry, 1996; Banerjee & Deshpande, 2016). The multiple isoforms of α-carbonic anhydrases, the family found in animals, are labeled CAI to CAXV and are differential expressed among tissues and cell types (Tarun et al., 2003). Mechanisms of CO_2 detection may respond to CO_2 directly, to bicarbonate ions, or to protons from the carbonic anhydrase reaction (Makino et al., 2019) (Figure 1A).

In insects, CO_2 directly activates gustatory receptors, a receptor family required for taste and pheromone detection (Kwon et al., 2007; Ning et al., 2016; Chu et al., 2020). *C. elegans* also detects CO_2 directly with isolated chemosensory BAG neurons (Smith et al., 2013). Alternatively, bicarbonate ions sometimes activate guanylate cyclases, opening cGMP-sensitive

ion channels and increasing cGMP (Sun et al., 2009). This is true in mice, where receptor-type guanylate cyclases GC-G and GC-D are activated by low concentrations of CO_2 (Kuhn, 2016), as well as in *C. elegans*, where chemosensory BAG neurons require the receptor-type guanylate cyclase GCY-9 for their response (Hallem et al., 2011).

Hydrogen ions produced by the carbonic anhydrase reaction may directly activate proton-sensitive channels. Transient receptor potential ankyrin subtype 1 (TRPA1) is one such channel, an evolutionarily conserved calcium channel that reacts to irritants, endogenous inflammatory agents, temperature, and weak acids (Bandell et al., 2004; Bautista et al., 2006; Wang et al., 2011). There is evidence in mice *in vitro* that the response of sensory neurons to CO_2 is mediated by TRPA1 channels activated by intracellular acidification from protons (Takahashi et al., 2008; Wang et al,, 2010; Wang et al., 2011). Otopetrin1 (OTOP1), the proton-sensitive proton channel required for sour taste in mammals (Teng et al, 2019; Tu et al, 2018), may also respond weak acids such as carbonic acid, a product of the carbonic anhydrase reaction (Teng et al., 2019). OTOP1 and OTOP3 are conserved across species with related genes in *Drosophila* (Tu et al., 2018).

Epithelial Na^+ channels (ENaCs), known as degenerins (DEG) in invertebrates, are a family of sodium channels involved in salt detection, sodium absorption, blood pressure regulation, and mechanotransduction (Kellenberger & Schild, 2002). Within this family are acid-sensing ion channels (ASICs), mammalian homologues of ENaCs activated by protons (Carattino & Montalbetti, 2020). The subtype ASIC3 is involved in chemoreception and opens at the physiologically relevant pHs of 7.3 to 6.7 (Osmakov et al., 2014; Li Xu, 2011), and could thus be involved in CO_2 detection. While ASIC blockage muted CO_2 responses in rats (Akiba et al., 2007), loss of function in mice did not affect CO_2 responses (Detwieler et al., 2018). ASIC homologues have been characterized in *C. elegans* (Rhoades et al, 2019), and there are many DEGs and ENaCs across invertebrates (Hanukoglu & Hanukoglu, 2016). Though there is no

evidence of an ASIC3-specific homologue in invertebrates, other ENaCs may be similarly involved with pH sensitivity, and by extension CO_2 detection, in invertebrates. Receptors that detect protons- TRPA1, OTOP1, and ENaCs- may also be involved in acid detection.

Here we investigate CO_2 and acid detection in the European Nightcrawler *Dendrobaena veneta* (previously known as *Eisenia hortensis*) using known mechanisms from other species as a template. *D. veneta* lives in burrows several cm below the ground and detects chemicals in the soil using sensory cells on its epithelium, either grouped into epithelial sensory organs (ESOs) or found alone as solitary chemoreceptor cells (Hess, 1925; Czoknya et al., 2005; Kizsler et al., 2012). These organs are likely candidates for the cellular receptors responsible for CO_2 detection and acid detection.

There is some evidence of these mechanisms in *D. veneta*. Our analysis of an epithelial transcriptome indicates that homologues to α-carbonic anhydrase, guanylate cyclase, TRPA1, ENaCs, and OTOP1 are expressed. Earthworms likely have functioning TRPA1 channels as they show behavioral aversion to TRPA1 activators (Silver et al., 2018). We expected high concentrations of CO_2 to be noxious to earthworms as in other species, and hypothesized that carbonic anhydrases, guanylate cyclases, TRPA1, ENaCs, and OTOPs may be involved with CO_2 detection in earthworms.

Materials and Methods

Earthworms

D. veneta earthworms were housed in plastic bins (approximate volume 40L) filled half-way with moist top soil covered with paper. The bins were maintained at room temperature with two light sources placed above the bins on a 12-12 light-dark cycle. The worms were watered with 250 ml of water poured over the newspaper twice a week, and fed with approximately 5 g

of “Purina Worm Chow” once a week. Only adult earthworms, identified by their visible clitellum, were used in experiments.

Transcriptomics

The epithelium from the prostomium (1st segment) and 15th segment posterior to the clitellum (hereafter referred to as the mid-segment) were quickly dissected free from the underlaying muscle and flash frozen on glass depression slides that had been placed on dry ice. Once frozen solid, the tissue was transferred into 1.5 mL LoBind microcentrifuge tubes (Eppendorf) where it was crushed with a plastic pedestal; both items were placed on dry ice to maintain their freezing temperature during this process. Refrigerated TRIzol Solution (1mL, Thermo Fisher Scientific) was added, and tissue was further macerated until no intact fragments were visible. Subsequently, RNA was isolated from the tissue-TRIzol mixture using the manufacturer’s standard chloroform extraction and isopropanol precipitation protocol. RNA concentration and integrity was verified using a bioanalyzer (Agilent). This protocol was developed because the earthworm epithelium was surprisingly durable, and other standard methods for tissue disruption (e.g. tissue homogenizers and column systems) failed to yield enough mRNA for sequencing. Pooled total RNA from the prostomium (n = 3) and mid-segment (n = 3) were used for these experiments, each pool contained tissue from 3 individuals (e.g. tissue was taken from 9 individual earthworms for these experiments).

RNA libraries were prepared from total RNA using the Kapa Stranded mRNA-Seq library prep kit, and 150 bp paired-end sequencing was performed on an Illumina HiSeq 4000 at Duke University’s Center for Genomic and Computational Biology (Durham, NC). Trimmomatic v0.36 (Bolger et al, 2014) was used to filter raw reads and to remove Illumina adaptors (4bp, mean Q30). *De novo* transcriptome assembly was performed by processing the filtered reads with Trinity v.2.5.1 (Haas et al., 2013), and the resulting transcripts were annotated with Trinotate

v.3.2.2 (Bryant et al., 2017) using the recommended settings. To develop gene candidate lists, the resulting Trinotate database was filtered for transcripts that were predicted to code for protein and contained one of the following terms: “carbonic anhydrase,” “gustatory receptor” “acid sensing ion channel,” “ASIC,” “guanylate cyclase,” “otopetrin,” “transient receptor potential,” or “TRPA.” These results were then confirmed and collected into candidate lists via human curation and are provided as used for analysis in Supplemental Material 1. Cladograms depicting the similarity of the predicted protein sequence for each group of candidate transcripts were constructed with R (R Core Team, 2021) using the following packages: ggtree (Yu et al, 2017), msa (Bodenhofer et al., 2015), seqinr (Charif et al., 2007), tidyverse (Wickham et al., 2019). Relevant code for reproducing these methods is available on Github and sequencing data has been uploaded to the NCBI sequence read archive.

CO_2 Aversion

Earthworms excrete exudate in response to noxious stimuli (Heredia et al., 2008). Given that high concentrations of CO_2 are aversive in most species, we predicted that degree of exudate production would reflect CO_2 detection and relative aversiveness. To perform the exudate assay, we first gently rinsed the earthworms in tap water and placed them in glass containers with moist paper towels to deprive them of soil and allow their digestive tract to empty. After 24 hours, a worm was placed in a glass petri dish with pre-weighed filter paper at the bottom and folded up the sides, and the dish was sealed with parafilm. The parafilm was punctured twice, and the dish was then saturated with air containing some percentage of CO_2 through a nozzle inserted through the parafilm. After one minute, the filter paper was immediately removed and weighed, and the weight of the exudate excreted at that time was calculated (Figure 1B).

Using this method, we tested responses to atmospheric CO_2, 25% CO_2, 50% CO_2, 75% CO_2, and 100% CO_2 and analyzed the data with a one-way ANOVA and a TukeysHSD. Varying percentages of CO_2 were obtained by combining different flow rates of room air and 100% CO2 using rotameters and a bubble flow meter for a final flow rate of approximately 32 ml/s for all trials. In this assay, 0% CO_2 represents room air, which typically has 400-1,000 ppm CO_2 (approximately 0.04%), 25% CO_2 includes approximately 250,525 ppm CO_2, 50% includes approximately 500,350 ppm CO_2, 75% includes approximately 750,175 ppm CO_2, and 100% includes approximately 1,000,000 ppm CO_2.

Pharmacology

After determining dosage response to CO_2, we repeated the assay after treatment with the inhibitors and blockers described in Table 1. For these treatments, the earthworms were placed in a 10 ml conical tube filled with 5 ml of the blocker prior to the experiment. After 10 minutes, they were removed from the tube and gently dried with a paper towel before being placed in the assay. The TRPA1 activator AITC, which we have previously showed to be aversive in *D. veneta* (Smith, 2019) and *Lumbricus terrestris* (Silver et al., 2019), was used as a positive control. In these trials, 500 ul of 500 mM AITC (allyl isothiocyanate) was pipetted onto a strip of filter paper placed in a 10 ml pipette and air was flown through the pipette into the assay chamber. The data were analyzed with two-way ANOVAs and TukeysHSDs.

Organic Acids

We also use the Exudate Assay to study the responses of earthworms to weak organic acids, including formic acid, acetic acid, and propionic acid (Fisher Scientific) at varying concentrations. For these trials, 250 ul of acid was pipetted onto a strip of filter paper placed in a 10 ml pipette, and air was flown through the pipette into the assay chamber. These trials were

repeated after exposure to the sodium channel and ASIC blocker amiloride using the procedure described above. These data were analyzed using two-way ANOVAs.

Results

Transcriptomics

The assembled *D. veneta* epithelial transcriptome contained 36 protein coding transcripts which were annotated as carbonic anhydrase (CA) homologs (Figure 2). The presence of CA mRNA supports the idea that these enzymes are involved in an earthworms ability to detect CO_2 concentration. Particularly of note are homologs to CA6 one of the only known secreted CA isoforms which is found in saliva and respiratory epithelium surface liquids of many other species. We queried our transcriptome for genes known to be involved in the detection of CO_2 and the various ions associated with carbonic acid and found many. However, we did not find any transcripts which annotated as homologs of the ionotropic gustatory receptor family. To ensure that our filtering criteria were not artifactually eliminating this gene family, we filtered our annotated transcriptome for any occurrence of the term “gustatory” and did not prefilter for protein-coding transcripts. Automated gene annotation pipelines can undercount ionotropic sensory receptors (Agnihotri et al., 2016; McKenzie et al., 2016; McKenzie & Kronauer, 2018), but it would be uncommon for there to be no evidence of transcripts corresponding to ionotropic gustatory receptors if they were enriched in the epithelial tissue we sequenced. Conversely, multiple unique transcripts annotated as acid-sensing ion channels (Figure 3), receptor-type guanylate cyclases (Figure 4), otopetrins (Figure 5), and TRPA1s (Figure 6). We thus attempted to test if any of these mechanisms were involved in the earthworm’s response to noxious levels of CO_2.

CO_2 Aversion

Earthworms excreted the most exudate in response to 100% CO_2. Over the course of the one-minute assay, earthworms first excreted clear liquid, and then a thicker pale green substance. Levels of movement varied between earthworms. Earthworms excreted more exudate with increasing concentrations of CO_2 in a dosage-dependent manner ($p<.0001$ two-way ANOVA), where concentrations of 0%, 25%, 50%, 75%, and 100% were tested (Figure 1C). Compared to these results, significantly more exudate was excreted when the earthworms were rinsed with deionized water before the experiment ($p<.01$, two-way ANOVA).

Pharmacology

This assay was repeated with 0%, 50%, and 100% CO_2 after treatment with blockers (Table 1). Of the carbonic anhydrase inhibitors, acetazolamide (general CA inhibitor, $p<.001$) and indisulam (CAIX/XII inhibitor, $p<.001$) significantly muted the response (Figure 7A). Of the receptor blockers, amiloride (ENaC blocker, $p<.0001$), diminazene aceturate (ASIC3 blocker, $p<.0001$), and ruthenium red (Ca2+ channel blocker, $p<.01$) significantly muted the response (Figure 7B). All statistics were generated by a two-way ANOVA with an alpha=.01, and a follow-up TukeysHSD test for these blockers revealed a significant difference in exudate excretion in response to blocker concentration for at least one concentration of CO_2 (Figure 7). HC030013 (TRPA1 channel blocker, $p<.05$), methylene blue (guanylate cyclase inhibitor, $p<.05$), S4 (CAIX inhibitor, $p<.05$), and ZnCl2 (OTOP1 blocker, $p<.05$) produced p-values below .05, but follow-up TukeysHSD tests produced no significant p-values, and these effects were determined to be non-significant. U-104 (CAIX/XII, $p>0.05$) and topiramate (CAII/IV, $p>0.05$) also did not significantly mute the response. Blocker trials were compared to trials with the blocker's respective vehicle (water, methyl cellulose, or 1% DMSO), because vehicles alone produced significantly increased responses (Figure 1A).

To control for effects of the blockers on the mechanisms of exudate release rather than detection of CO_2, the positive control AITC was tested after exposure to acetazolamide, amiloride, diminazene aceturate, indisulam, and HC030013 (Figure 8). Acetazolamide ($p>.05$), 1 mM amiloride ($p>.05$), and indisulam ($p>.05$) did not significantly mute the response to AITC by a TukeysHSD test, but HC030013 ($p<0.0001$), 5 mM amiloride ($p<0.0001$), .05 mM diminazene aceturate ($p<0.01$), and .1 mM diminazene aceturate ($p<0.01$) did. HC030013 and amiloride are both TRPA1 blockers (Banke, 2011; Eid et al, 2008) and predictably blocked AITC detection. HC030013 and indisulam were both compared to water vehicle data rather than their respective vehicles methyl cellulose and 1% DMSO; we do not expect that this affects the significance, as both vehicles produced larger responses to CO_2 than water. The vehicle for AITC, mineral oil, produced no significant response on its own when compared to 0% CO2 ($p=1.00$).

Organic Acids

Earthworms also excreted significantly more exudate in response to increasing concentrations of formic acid, acetic acid, and propionic acid ($p<.0001$, two-way ANOVA) (Figure 9B). This response was significantly muted after treatment with the sodium channel and ASIC blocker amiloride ($p<.0001$, two-way ANOVA) (Figure 9C).

Discussion

The Exudate Assay

This study provides initial evidence of the molecular mechanisms behind CO_2 detection in earthworms, providing insight into how earthworms detect chemicals in their environment, and contributing to ongoing investigations into mechanisms of CO_2 detection across species.

The chemosensory capabilities of earthworms were famously discussed by Darwin and have been the subject of anatomical, physiology and most often ecological studies since that time. However, there is comparative dearth of publications that examine earthworm biology with an eye towards identifying the molecular mechanisms that mediate their physiology and behavior (Stürzenbaum et al., 2009). In fact, we believe that this study is the first to use modern sequencing technologies to elucidate the molecular mechanism responsible for any type of earthworm chemosensation.

Exudate acts as an alarm signal to other earthworms and is attractive to some predators such as garter snakes (Jiang et al., 1990). Protein and carbohydrate-rich mucus vesicles containing auto-fluorescent membrane-bound chloragosome granules are excreted from between the earthworm's segments and lubricated by coelomic fluid (Roots and Johnston, 1966; Heredia et al., 2008; Zhang et al., 2016; Guhra et al., 2020). Studies in the closely related *Eisenia fetida* show that the vesicles form strands outside the body, which differs from the globules we observed in *D. veneta* (Heredia et al., 2008). Exudate composition also differs chemically between earthworm species, including in *D. veneta* α-nicotinamide riboside (the main aromatic compound) and the organic acids fumarate, succinate, malate, and α-ketoglutarate (Bundy et al., 2001; Rochfort et al., 2017). Our transcriptome data suggest that homologs to secreted CA6 may be one component of the exudate (Figure 2) and the presence of CA6. Because earthworms excrete exudate in response to noxious stimuli (Heredia et al., 2008; Rivera et al., 2020), we used the amount of exudate produced as a proxy for aversion.

CO2 Aversion and Adaptations

CO_2 is noxious to earthworms in a dosage-dependent manner. Many species find CO_2 noxious at high concentrations, including rats, nematodes, and fruit flies (Hallem & Sternburg, 2008; Breugel et al., 2018; Améndola & Weary, 2019). High concentrations of CO2 also

anesthetize many species, including rats and fruit flies (Seiger & Kink, 1993; Danneman & Walshaw, 1997), but we did not observe this in earthworms even with 100% CO2. Low concentrations of CO_2 (ex: 25%) produced no significant response in earthworms, though such concentrations are noxious in other species including rats (25%; Améndola & Weary, 2019), nematodes (10%; Hallem & Sternburg, 2008), and fruit flies (5% when not foraging; Breugel et al, 2018). Earthworms may be resistant to high CO_2 concentrations due to high exposure in their environment; mechanistic adaptations may underlie such resistance. Naked-mole rats have a proton-insensitive ASIC3 channel among other adaptations to their high-CO_2 environment (Schuhmacher et al, 2018); earthworms may have similar adaptations. Concentrations as high as 45% have been used in human irritation studies, suggesting similar tolerance, although in a much larger animal (Shusterman Avila, 2003; Hummel et al., 1998).

Low concentrations of CO_2 may also be appetitive rather than aversive; this is true of mosquitoes and, when in a foraging state, fruit flies (Breugel et al., 2018; Spanoudis et al., 2020). Earthworms feed on soil, gaining nutrients from decaying organic matter, bacteria, nematodes, and other microfauna (Curry & Schmit, 2007), many of which emit CO_2. Low concentrations may also use different mechanisms than aversive high concentrations. However, insects like mosquitoes and fruit flies detect CO_2 through ionotropic gustatory receptors which we found no evidence of in the *D. veneta* transcriptome.

Earthworms rinsed with deionized water produced more exudate in response to CO_2 compared to untreated worms. We hypothesize that the water washed off the earthworms' mucus, the liquid found on earthworms' epithelium under basal conditions. Mucus keeps the skin moist for respiration, aids with locomotion, and acts as a buffer (Zhang et al, 2016; Schrader et al., 1994). Mucus may thus neutralize the low-pH environment created from CO_2 and water by carbonic anhydrase. Because treatment with water also increased the aversive response to AITC, mucus likely also physically blocked the epithelium from irritants. It is

somewhat unclear to what extent mucus and exudate are the same. Many studies electrically or chemically stimulate earthworms to release exudate in order to collect and study mucus (Jiang et al., 1990; Zhang et al., 2016), and *E. fetida* excretes small amounts of exudate proteins under basal conditions (Rivera et al, 2020; Heredia et al, 2008). A scant number of studies have thoroughly examined the composition and the chemical properties of earthworm mucus and exudate, which make the topic easy to speculate on. We predict that exudate production in response to irritants could serve a similar function as mucus in buffering and blocking irritants. Alternatively, the water could allow more CO_2 to dissolve and be converted to bicarbonate and protons by carbonic anhydrase, producing more protons to activate receptors. These competing hypotheses emphasize the need for more research focusing on the molecular mechanisms that underlie earthworm chemical senses.

Mechanisms of CO_2 *Detection*

While we acknowledge that these concentrations of CO_2 are much higher than what an earthworm is likely to encounter in its subterranean environment (up to 13% CO_2) (Amundson & Davidson, 1990), the non-ecological concentrations used here allowed for investigation of the mechanisms behind CO_2 aversion. Repetition of the exudate assay after exposure to blockers demonstrated that carbonic anhydrase is necessary for aversion to high concentrations of CO_2, as the general carbonic anhydrase inhibitor acetazolamide and the carbonic anhydrase IX/XII inhibitor indisulam both significantly muted responses to CO_2. Earthworms may thus have CAIX and CAXII orthologues. That the CAIX/XII inhibitor U-104 and CAIX inhibitor S4 had little effect on CO_2-induced irritation may contradict this theory or at least suggests that these CAIX/XII orthologues have diverged in such a way that these blockers are no longer effective at inhibiting the enzyme. In mammals, CAXII, CAII, CAVB, and 5 CAIV are found in the human nasal mucosa (Tarun et al., 2003), and CAIV is required for sour taste responses to carbon dioxide (Chandrashekar et al., 2009), but CAII and CAIV orthologues are likely not involved in

earthworm CO_2 detection, as CAII/IV inhibitor topiramate had no significant effect. Alternatively, earthworm CAII homologs may be so divergent from those of the other organisms that topiramate has previously been tested on that the inhibitor simply does not have an effect on earthworm CA II. Multiple carbonic anhydrase isoforms may contribute to earthworms' response to CO_2; this would explain the larger effect by the general carbonic anhydrase inhibitor acetazolamide compared to the inhibitors of single isoforms. Additionally, given the relatively low percentage identity of earthworm CA to its homologs, that acetazolamide retained its effectiveness on muting the earthworms response to CO_2 validates it at a broad spectrum CA inhibitor. The biological redundancy observed in the earthworms response to CO_2 is likely indicative of the general importance of CO_2 detection to all animals or could be evidence that carbonic anhydrases are of particular importance to the survivability of earthworms. That carbonic anhydrase is required for a response to CO_2 suggests that earthworms' sensory receptors detect protons or bicarbonate rather than CO_2.

Guanylate cyclases, OTOP channels, and TRPA1 channels are likely not required for CO2 detection in *D. veneta*, their blockers did not significantly affect earthworms' responses to CO2. Because carbonic anhydrase did mute the response, it is also unlikely that CO_2-specific sensory cells are required. Amiloride, however, did mute the exudate response to CO_2, suggesting that an epithelial sodium channel is required for CO_2 detection and aversion. The ASIC3 blocker diminazene aceturate also muted responses to CO_2, but the role of ASIC3 cannot be confirmed because it also muted the response to the positive control AITC, suggesting that it may impact the mechanism of exudate excretion rather than CO_2 detection. High concentrations of amiloride also muted responses to AITC, but because the ENaC blocker amiloride is also a TRPA1 blocker at high concentrations (Banke, 2011), this response was somewhat expected. Low concentrations of amiloride muted responses to CO_2 but not AITC,

further suggesting the role of the ENaC superfamily in CO_2 detection. This is corroborated by the responses to organic acids, which were also muted by amiloride.

Conclusions

Earthworms are critical to many terrestrial ecosystems, yet we know little about how they make decisions about the chemicals in their environment. CO_2 is a critical signaling molecule that earthworms encounter at high concentrations. This research could thus contribute to a necessary understanding of what attracts and repels earthworms, which has potential applications in agriculture and invasive species management. Research on responses to CO_2 may be of particular importance in the context of climate change: as CO_2 concentrations in the atmosphere increase, CO_2 concentrations in the soil may increase as well. These results suggest that increasing concentrations of CO_2 in the soil won't be aversive to earthworms, demonstrating their potential resilience to a changing environment. There are also potential applications in the assessment and treatment of acidic soil, as our data supports previous studies describing earthworm mucus as an effective buffer (Zhang et al, 2016; Schrader et al, 1994).

These data may also provide insight into CO_2 detection and chemosensation across species. Because earthworms respire (e.g. "breathe") through their skin, their entire body is a respiratory epithelium (Karaca, 2011). This makes them an excellent model for chemosensation in the respiratory epithelium across invertebrate and vertebrate species, including CO_2 and acid detection. Our investigation of this topic has contributed to our understanding of the mechanisms earthworms use to detect carbon dioxide and provides yet another example of how these molecular mechanisms are highly conserved among metazoa.

Supplementary material

S1: SmithEtal2023-canidates.xlsx - Excel file containing full Trinotate annotations for candidate transcripts in this study. Each set of candidate transcripts is in a separate tab/worksheet of this file.

Data availability statements

The transcriptome datasets generated for this study can be found in the NIH's National Library of Medicine's National Center for Biotechnology Information's Sequence Read Archive (https://www.ncbi.nlm.nih.gov/sra). The accession number for this data set is PRJNAXXXXXX.

Funding

This work was supported by NSF IOS1355097 to EJ, and grants from the Wake Forest University Center for Molecular Signaling to EJ, WS and CS. Additional funds were provided by the Wake Forest University Provost's Office and Wake Forest University's Department of Biology.

Acknowledgments

Computations for this study were performed using the Wake Forest University (WFU) High-Performance Computing Facility, a centrally managed computational resource available to WFU researchers including faculty, staff, students, and collaborators (Information Systems and Wake Forest University, 2021). Some data and text included in this manuscript originally appeared in ES's master's thesis (Smith, 2021).

References

Akiba, Y., Mizumori, M., Kuo, M., Ham, M., Guth, P.H., Engel, E., Kaunitz, J.D. (2008). CO2 chemosensing in rat oesophagus. Gut 57, 1654–1664. https://doi.org/10.1136/gut.2007.144378

Améndola L, Weary DM. (2019). Evidence for consistent individual differences in rat sensitivity to carbon dioxide. PloS one. 14:e0215808. https://doi.org/10.1371/journal.pone.0215808

Amundson, R.G., Davidson, E.A. (1990). Carbon dioxide and nitrogenous gases in the soil atmosphere. Journal of Geochemical Exploration. 38, 13–41. https://doi.org/10.1016/0375-6742(90)90091-N

Bandell, M., Story, G.M., Hwang, S.W., Viswanath, V., Eid, S.R., Petrus, M.J., Earley, T.J., Patapoutian, A. (2004). Noxious cold ion channel TRPA1 is activated by pungent compounds and bradykinin. Neuron. 41, 849–857. https://doi.org/10.1016/s0896-6273(04)00150-3

Banerjee, S., Deshpande, P.A. (2016). On origin and evolution of carbonic anhydrase isozymes: A phylogenetic analysis from whole-enzyme to active site. Computational Biology and Chemistry. 61, 121–129. https://doi.org/10.1016/j.compbiolchem.2016.01.003

Banke, T.G. (2011). The dilated TRPA1 channel pore state is blocked by amiloride and analogues. Brain Res. 1381, 21–30. https://doi.org/10.1016/j.brainres.2011.01.021

Bautista, D.M., Jordt, S.-E., Nikai, T., Tsuruda, P.R., Read, A.J., Poblete, J., Yamoah, E.N., Basbaum, A.I., Julius, D. (2006). TRPA1 Mediates the Inflammatory Actions of Environmental Irritants and Proalgesic Agents. Cell. 124, 1269–1282. https://doi.org/10.1016/j.cell.2006.02.023

Bodenhofer U., Bonatesta E., Horejs-Kainrath C., Hochreiter S. (2015). “msa: an R package for multiple sequence alignment.” Bioinformatics. 31, 3997–3999. doi:10.1093/bioinformatics/btv494.

Bolger, A. M., Lohse, M., & Usadel, B. (2014). Trimmomatic: A flexible trimmer for Illumina Sequence Data. Bioinformatics, btu170.

Bryant D.M., Johnson K., DiTommaso T., Tickle T., Couger M.B., Payzin-Dogru D., Lee T.J., Leigh N.D., Kuo T.H., Davis F.G., Bateman J., Bryant S., Guzikowski A.R., Tsai S.L., Coyne S., Ye W.W., Freeman R.M. Jr, Peshkin L., Tabin C.J., Regev A., Haas B.J., Whited J.L. (2017) A Tissue-Mapped Axolotl De Novo Transcriptome Enables Identification of Limb Regeneration Factors. Cell Rep. 18(3):762-776. doi: 10.1016/j.celrep.2016.12.063.

Bundy, J.G., Osborn, D., Weeks, J.M., Lindon, J.C., Nicholson, J.K. (2001). An NMR-based metabonomic approach to the investigation of coelomic fluid biochemistry in earthworms under toxic stress. FEBS Letters. 500, 31–35. https://doi.org/10.1016/S0014-5793(01)02582-0

Carattino, M.D., Montalbetti, N. (2020). Acid-sensing ion channels in sensory signaling. Am J Physiol Renal Physiol. 318, F531–F543. https://doi.org/10.1152/ajprenal.00546.2019

Chandrashekar, J., Yarmolinsky, D., von Buchholtz, L., Oka, Y., Sly, W., Ryba, N.J.P., Zuker, C.S. (2009). The Taste of Carbonation. Science. 326, 443–445. https://doi.org/10.1126/science.1174601

Charif D., Lobry J. (2007). SeqinR 1.0-2: a contributed package to the R project for statistical computing devoted to biological sequences retrieval and analysis. In Bastolla U, Porto M, Roman H, Vendruscolo M (eds.), Structural approaches to sequence evolution: Molecules, networks, populations, series Biological and Medical Physics, Biomedical Engineering. 207-232. Springer Verlag, New York. ISBN : 978-3-540-35305-8.

Chu, X., Kc, P., Ian, E., Kvello, P., Liu, Y., Wang, G.R., Berg, B.G. (2020). Neuronal architecture of the second-order CO2 pathway in the brain of a noctuid moth. Sci Rep. 10, 19838. https://doi.org/10.1038/s41598-020-76918-1

Csoknya, M., Takács, B., Koza, A., Dénes, V., Wilhelm, M., Hiripi, L., Kaslin, J., Elekes, K. (2005). Neurochemical characterization of nervous elements innervating the body wall of earthworms (Lumbricus, Eisenia): immunohistochemical and pharmacological studies. Cell Tissue Res. 321, 479–490. https://doi.org/10.1007/s00441-005-1134-4

Cummins, E.P., Strowitzki, M.J., Taylor, C.T. (2020). Mechanisms and Consequences of Oxygen and Carbon Dioxide Sensing in Mammals. Physiological Reviews. 100, 463–488. https://doi.org/10.1152/physrev.00003.2019

Curry, J.P., Schmidt, O. (2007). The feeding ecology of earthworms – A review. Pedobiologia. 50, 463–477. https://doi.org/10.1016/j.pedobi.2006.09.001

Danneman, P.J., Stein, S., Walshaw, S.O. (1997). Humane and practical implications of using carbon dioxide mixed with oxygen for anesthesia or euthanasia of rats. Lab Anim Sci. 47, 376–385.

Detweiler, N.D., Vigil, K.G., Resta, T.C., Walker, B.R., Jernigan, N.L. (2018). Role of acid-sensing ion channels in hypoxia- and hypercapnia-induced ventilatory responses. PLOS ONE. 13:e0192724. https://doi.org/10.1371/journal.pone.0192724

Edwards, C. (2004). Earthworm Ecology. 2nd. Danvers, MA: CRC Press LLC. Chapter 1, The Importance of Earthworms as Key Representatives of the Soil Fauna, p. 3-9

Eid, S.R., Crown, E.D., Moore, E.L., Liang, H.A., Choong, K.-C., Dima, S., Henze, D.A., Kane, S.A., Urban, M.O. (2008). HC-030031, a TRPA1 selective antagonist, attenuates inflammatory- and neuropathy-induced mechanical hypersensitivity. Mol Pain. 4, 48. https://doi.org/10.1186/1744-8069-4-48

Fang, X., Seim, I., Huang, Z., Gerashchenko, M.V., Xiong, Z., Turanov, A.A., Zhu, Y., Lobanov, A.V., Fan, D., Yim, S.H., Yao, X., Ma, S., Yang, L., Lee, S.-G., Kim, E.B., Bronson, R.T., Šumbera, R., Buffenstein, R., Zhou, X., Krogh, A., Park, T.J., Zhang, G., Wang, J., Gladyshev,

V.N. (2014). Adaptations to a subterranean environment and longevity revealed by the analysis of mole rat genomes. Cell Rep. 8, 1354–1364. https://doi.org/10.1016/j.celrep.2014.07.030

Guhra, T., Stolze, K., Schweizer, S., Totsche, K.U. (2020). Earthworm mucus contributes to the formation of organo-mineral associations in soil. Soil Biology and Biochemistry. 145, 107785. https://doi.org/10.1016/j.soilbio.2020.107785

Haas B.J., Papanicolaou A., Yassour M., Grabherr M., Blood P.D., Bowden J., Couger M.B., Eccles D., Li B., Lieber M., Macmanes M.D., Ott M., Orvis J., Pochet N., Strozzi F., Weeks N., Westerman R., William T., Dewey C.N., Henschel R., Leduc R.D., Friedman N., Regev A. (2013) De novo transcript sequence reconstruction from RNA-seq using the Trinity platform for reference generation and analysis. Nat Protoc. 8, 1494-1512. doi: 10.1038/nprot.2013.084.

Hallem E.A., Spencer W.C., McWhirter R.D., Zeller G., Henz S.R., Rätsch G., Miller D.M., 3rd Horvitz H.R., Sternberg P.W., Ringstad, N. (2011). Receptor-type guanylate cyclase is required for carbon dioxide sensation by *Caenorhabditis elegans*. Proceedings of the National Academy of Sciences of the United States of America. 108, 254–259. https://doi.org/10.1073/pnas.1017354108

Hallem, E.A., Sternberg, P.W. (2008). Acute carbon dioxide avoidance in Caenorhabditis elegans. Proc Natl Acad Sci U S A. 105, 8038–8043. https://doi.org/10.1073/pnas.0707469105

Hanukoglu, I., Hanukoglu, A. (2016). Epithelial sodium channel (ENaC) family: Phylogeny, structure-function, tissue distribution, and associated inherited diseases. Gene. 579, 95–132. https://doi.org/10.1016/j.gene.2015.12.061

Henry, R.P. (1996). Multiple Roles of Carbonic Anhydrase in Cellular Transport and Metabolism. Annu. Rev. Physiol. 58, 523–538. https://doi.org/10.1146/annurev.ph.58.030196.002515

Heredia, R.B., Dueñas, S., Castillo, L., Ventura, J.J., Silva Briano, M., Posadas del Rio, F., Rodríguez, M.G. (2008). Autofluorescence as a tool to study mucus secretion in Eisenia foetida. Comparative Biochemistry and Physiology Part A: Molecular & Integrative Physiology, Fifth Special Issue of CBP dedicated to “The Face of Latin American Comparative Biochemistry and Physiology”. 151, 407–414. https://doi.org/10.1016/j.cbpa.2007.01.726

Hess, W.N. (1925). Nervous system of the earthworm, lumbricus terrestris L. Journal of Morphology. 40, 235–259. https://doi.org/10.1002/jmor.1050400203

Hummel, T., Kraetsch, H.G., Pauli, E., Kobal, G. (1998). Responses to nasal irritation obtained from the human nasal mucosa. Rhinology. 36, 168–172.

Information Systems and Wake Forest University. (2021) WFU High Performance Computing Facility. https://doi.org/10.57682/g13z-2362.

Jiang, X.C., Inouchi, J., Wang, D., Halpern, M. (1990). Purification and characterization of a chemoattractant from electric shock-induced earthworm secretion, its receptor binding, and

signal transduction through the vomeronasal system of garter snakes. Journal of Biological Chemistry. 265, 8736–8744. https://doi.org/10.1016/S0021-9258(19)38950-1

Karaca, A. (2011). Biology of Earthworms, Soil Biology. Springer, Berlin, Heidelberg, pp. 141–158. https://doi.org/10.1007/978-3-642-14636-7_9

Kellenberger, S., Schild, L. (2002). Epithelial Sodium Channel/Degenerin Family of Ion Channels: A Variety of Functions for a Shared Structure. Physiological Reviews. 82, 735–767. https://doi.org/10.1152/physrev.00007.2002

Kiszler, G., Varhalmi, E., Berta, G., Molnar, L. (2012). Organization of the sensory system of the earthworm Lumbricus terrestris (Annelida, Clitellata) visualized by DiI. Journal of Morphology. 273, 737–745. https://doi.org/10.1002/jmor.20018

Kuhn, M. (2016). Molecular Physiology of Membrane Guanylyl Cyclase Receptors. Physiological Reviews. 96, 751–804. https://doi.org/10.1152/physrev.00022.2015

Kwon J.Y., Dahanukar A., Weiss L.A., Carlson J.R. (2007) The molecular basis of CO2 reception in *Drosophila*. Proc Natl Acad Sci U S A. 104(9):3574-3578. doi: 10.1073/pnas.0700079104.

Li, W.-G., Xu, T.-L. (2011). ASIC3 Channels in Multimodal Sensory Perception. ACS Chem. Neurosci. 2, 26–37. https://doi.org/10.1021/cn100094b

Lindskog, S. (1997). Structure and mechanism of carbonic anhydrase. Pharmacology & Therapeutics. 74, 1–20. https://doi.org/10.1016/S0163-7258(96)00198-2

Makino, C.L., Duda, T., Pertzev, A., Isayama, T., Geva, P., Sandberg, M.A., Sharma, R.K. (2019). Modes of Accessing Bicarbonate for the Regulation of Membrane Guanylate Cyclase (ROS-GC) in Retinal Rods and Cones. eNeuro:6. https://doi.org/10.1523/ENEURO.0393-18.2019

Ning, C., Yang, K., Xu, M., Huang, L.-Q., Wang, C.-Z. (2016). Functional validation of the carbon dioxide receptor in labial palps of *Helicoverpa armigera* moths. Insect Biochemistry and Molecular Biology. 73, 12–19. https://doi.org/10.1016/j.ibmb.2016.04.002

Osmakov, D.I., Andreev, Ya.A., Kozlov, S.A. (2014). Acid-sensing ion channels and their modulators. Biochemistry Moscow. 79, 1528–1545. https://doi.org/10.1134/S0006297914130069

R Core Team (2021). R: A language and environment for statistical computing. R Foundation for Statistical Computing, Vienna, Austria. https://www.R-project.org/.

Reed, E. M., O'Connor, M. O., Johnson, I. C., Silver, W. L., & Saunders, C. J. (2021). Dendrobaena veneta avoids ethyl pentanoate and ethyl hexanoate, two compounds produced by the soil fungus Geotrichum candidum. PeerJ, 9, e12148.

Rhoades, J.L., Nelson, J.C., Nwabudike, I., Yu, S.K., McLachlan, I.G., Madan, G.K., Abebe, E., Powers, J.R., Colón-Ramos, D.A., Flavell, S.W. (2019). ASICs Mediate Food Responses in an Enteric Serotonergic Neuron that Controls Foraging Behaviors. Cell. 176, 85-97.e14. https://doi.org/10.1016/j.cell.2018.11.023

Rochfort, S., Wyatt, M.A., Liebeke, M., Southam, A.D., Viant, M.R., Bundy, J.G. (2017). Aromatic metabolites from the coelomic fluid of *Eisenia earthworm* species. European Journal of Soil Biology. 78, 17–19. https://doi.org/10.1016/j.ejsobi.2016.11.008

Roots, B.I., Johnston, P.V. (1966). The lipids and pigments of the chloragosomes of the earthworm *Lumbricus terrestris.* L. Comp Biochem Physiol. 17, 285–288. https://doi.org/10.1016/0010-406x(66)90027-2

Schrader S. (1994). Influence of Earthworms on pH Conditions of Their Environment by Cutaneous Mucus Secretion, Zool, Anz. 233, 211-219

Scott, K. (2011). Out of thin air: Sensory detection of oxygen and carbon dioxide. Neuron. 69, 194–202. https://doi.org/10.1016/j.neuron.2010.12.018

Seiger, M.B., Kink, J.F. (1993). The effect of anesthesia on the photoresponses of four sympatric species of *Drosophila*. Behav Genet. 23, 99–104. https://doi.org/10.1007/BF01067559

Shams, I., Avivi, A., Nevo, E. (2005). Oxygen and carbon dioxide fluctuations in burrows of subterranean blind mole rats indicate tolerance to hypoxic–hypercapnic stresses. Comparative Biochemistry and Physiology Part A: Molecular & Integrative Physiology. 142, 376–382. https://doi.org/10.1016/j.cbpa.2005.09.003

Shusterman, D., Avila, P.C. (2003). Real-time Monitoring of Nasal Mucosal pH During Carbon Dioxide Stimulation: Implications for Stimulus Dynamics. Chemical senses. 28, 595–601. https://doi.org/10.1093/chemse/bjg050

Silver, W. L., Kim, A. H., Kim, E. Y., & Saunders, C. J. (2019). A novel T-maze assay to evaluate chemical irritants on Lumbricus terrestris. Applied Soil Ecology, 133, 186-189.

Silver, W., Kim, E., Krivda, K., Robertson, J., Smith, K. (2018). Are TRPA1 Channels Involved in the Detection of Chemical Irritants by the Earthworm, *Eisenia hortensis*?. Chemical Senses 43, 543 https://academic.oup.com/chemse/article/43/4/e1/4925423?searchresult=1

Smith, E.J. (2021) Title. [Mechanisms of carbon dioxide detection in the earthworm *Eisenia hortensis*].. [master's thesis]. [Winston-Salem (NC)]: Wake Forest University

Smith, E.St.J., Martinez-Velazquez, L., Ringstad, N. (2013). A Chemoreceptor That Detects Molecular Carbon Dioxide. J Biol Chem. 288, 37071–37081. https://doi.org/10.1074/jbc.M113.517367

Smith, K. (2019) A Molecular Investigation of chemesthesis in *Eisenia hortensis* through analysis of transient receptor potential channels. [dissertation/master's thesis]. [Winston-Salem (NC)]: Wake Forest University

Spanoudis, C.G., Andreadis, S.S., Bray, D.P., Savopoulou-Soultani, M., Ignell, R. (2020). Behavioural response of the house mosquitoes *Culex quinquefasciatus* and *Culex pipiens molestus* to avian odours and its reliance on carbon dioxide. Medical and Veterinary Entomology. 34, 129–137. https://doi.org/10.1111/mve.12429

Stürzenbaum, S. R., Andre, J., Kille, P., & Morgan, A. J. (2009). Earthworm genomes, genes and proteins: the (re) discovery of Darwin's worms. Proceedings of the Royal Society B: Biological Sciences. 276(1658), 789-797.

Suh, G.S.B., Wong, A.M., Hergarden, A.C., Wang, J.W., Simon, A.F., Benzer, S., Axel, R., Anderson, D.J. (2004). A single population of olfactory sensory neurons mediates an innate avoidance behaviour in Drosophila. Nature. 431, 854–859. https://doi.org/10.1038/nature02980

Sun, L., Wang, H., Hu, J., Han, J., Matsunami, H., Luo, M. (2009). Guanylyl cyclase-D in the olfactory CO2 neurons is activated by bicarbonate. PNAS. 106, 2041–2046. https://doi.org/10.1073/pnas.0812220106

Takahashi, N., Mizuno, Y., Kozai, D., Yamamoto, S., Kiyonaka, S., Shibata, T., Uchida, K., Mori, Y. (2008). Molecular characterization of TRPA1 channel activation by cysteine-reactive inflammatory mediators. Channels. 2, 287–298. https://doi.org/10.4161/chan.2.4.6745

Tarun, A.S., Bryant, B., Zhai, W., Solomon, C., Shusterman, D. (2003). Gene Expression for Carbonic Anhydrase Isoenzymes in Human Nasal Mucosa. Chemical Senses. 28, 621–629. https://doi.org/10.1093/chemse/bjg054

Teng, B., Wilson, C.E., Tu, Y.-H., Joshi, N.R., Kinnamon, S.C., Liman, E.R. (2019). Cellular and Neural Responses to Sour Stimuli Require the Proton Channel Otop1. Current Biology. 29, 3647-3656.e5. https://doi.org/10.1016/j.cub.2019.08.077

Tu, Y.-H., Cooper, A.J., Teng, B., Chang, R.B., Artiga, D.J., Turner, H.N., Mulhall, E.M., Ye, W., Smith, A.D., Liman, E.R. (2018). An Evolutionarily Conserved Gene Family Encodes Proton-Selective Ion Channels. Science. 359, 1047–1050. https://doi.org/10.1126/science.aao3264

van Breugel, F., Huda, A., Dickinson, M.H. (2018). Distinct activity-gated pathways mediate attraction and aversion to CO2 in *Drosophila*. Nature. 564, 420–424. https://doi.org/10.1038/s41586-018-0732-8

Wickham H., Averick M., Bryan J., Chang W., McGowan L.D., François R., Grolemund G., Hayes A., Henry L., Hester J., Kuhn M., Pedersen T.L., Miller E., Bache S.M., Müller K., Ooms J., Robinson D., Seidel D.P., Spinu V., Takahashi K., Vaughan D., Wilke C., Woo K., Yutani H. (2019). Welcome to the tidyverse. Journal of Open Source Software. 4, 1686. doi:10.21105/joss.01686.

Wang, Y.Y., Chang, R.B., Allgood, S.D., Silver, W.L., Liman, E.R. (2011). A TRPA1-dependent mechanism for the pungent sensation of weak acids. J Gen Physiol. 137, 493–505. https://doi.org/10.1085/jgp.201110615

Wang, Y.Y., Chang, R.B., Liman, E.R. (2010). TRPA1 is a component of the nociceptive response to CO_2. J Neurosci. 30, 12958–12963. https://doi.org/10.1523/JNEUROSCI.2715-10.2010

Yu G., Smith D., Zhu H., Guan Y., Lam T.T. (2017). ggtree: an R package for visualization and annotation of phylogenetic trees with their covariates and other associated data. Methods in Ecology and Evolution. 8, 28-36. doi: 10.1111/2041-210X.12628, http://onlinelibrary.wiley.com/doi/10.1111/2041-210X.12628/abstract.

Zhang, D., Chen, Y., Ma, Y., Guo, L., Sun, J., Tong, J. (2016). Earthworm epidermal mucus: Rheological behavior reveals drag-reducing characteristics in soil. Soil and Tillage Research. 158, 57–66. https://doi.org/10.1016/j.still.2015.12.001

Figures and Tables

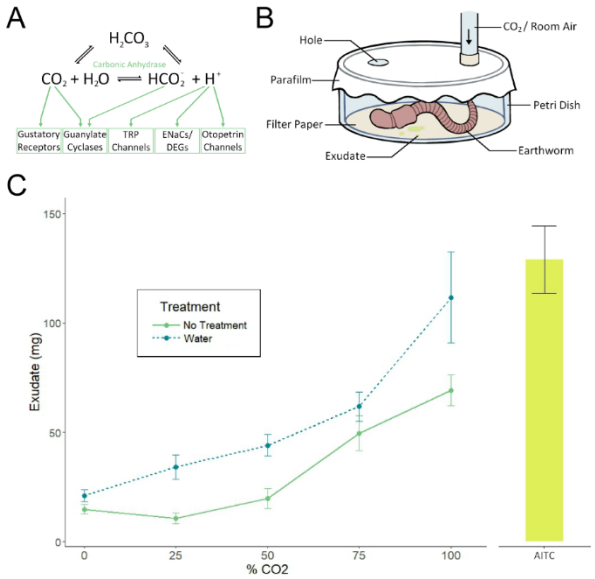

Figure 1. Mechanism of CO_2 detection and the exudate assay. (A) CO_2 + H2O ⟷ HCO_2- + H+ dissociation reaction catalyzed by carbonic anhydrase. The green arrows point to the potential mechanisms by which CO2 and its products could be detected.(B) Diagram of the exudate assay. Earthworms were placed in a sealed container filled with a volatile or gaseous chemical for one minute, and the amount of exudate produced in that time was recorded. (C) Earthworms excreted significantly more exudate in response to increasing concentrations of CO_2 ($p<.0001$, two-way ANOVA). Earthworms also excreted significantly more exudate in response to CO_2 if they were rinsed in deionized water prior to the assay ($p<.01$, two-way ANOVA). Air flowed over filter paper containing 500 ul of 500 mM AITC shown as a positive control for comparison.

Unique Carbonic Anhydrase (CA) Transcripts

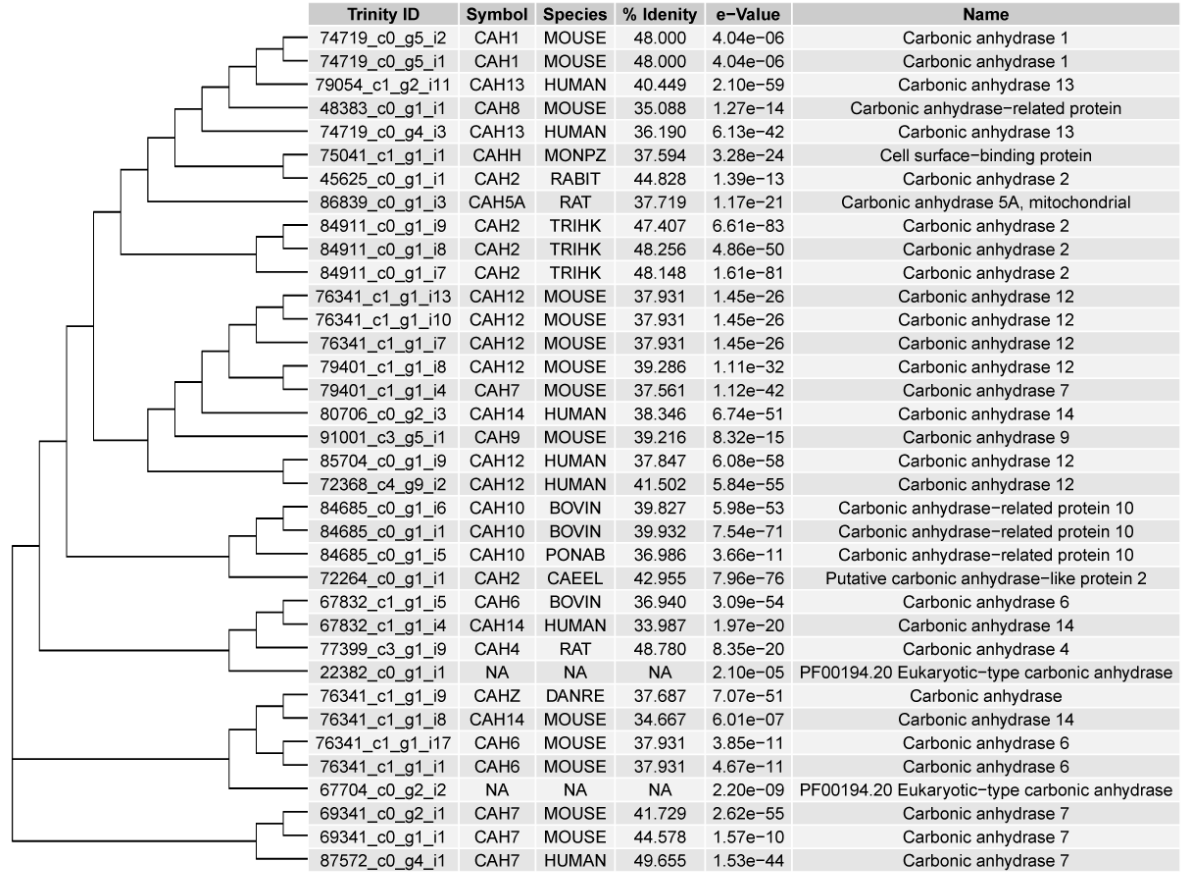

Trinity ID	Symbol	Species	% Idenity	e−Value	Name
74719_c0_g5_i2	CAH1	MOUSE	48.000	4.04e−06	Carbonic anhydrase 1
74719_c0_g5_i1	CAH1	MOUSE	48.000	4.04e−06	Carbonic anhydrase 1
79054_c1_g2_i11	CAH13	HUMAN	40.449	2.10e−59	Carbonic anhydrase 13
48383_c0_g1_i1	CAH8	MOUSE	35.088	1.27e−14	Carbonic anhydrase−related protein
74719_c0_g4_i3	CAH13	HUMAN	36.190	6.13e−42	Carbonic anhydrase 13
75041_c1_g1_i1	CAHH	MONPZ	37.594	3.28e−24	Cell surface−binding protein
45625_c0_g1_i1	CAH2	RABIT	44.828	1.39e−13	Carbonic anhydrase 2
86839_c0_g1_i3	CAH5A	RAT	37.719	1.17e−21	Carbonic anhydrase 5A, mitochondrial
84911_c0_g1_i9	CAH2	TRIHK	47.407	6.61e−83	Carbonic anhydrase 2
84911_c0_g1_i8	CAH2	TRIHK	48.256	4.86e−50	Carbonic anhydrase 2
84911_c0_g1_i7	CAH2	TRIHK	48.148	1.61e−81	Carbonic anhydrase 2
76341_c1_g1_i13	CAH12	MOUSE	37.931	1.45e−26	Carbonic anhydrase 12
76341_c1_g1_i10	CAH12	MOUSE	37.931	1.45e−26	Carbonic anhydrase 12
76341_c1_g1_i7	CAH12	MOUSE	37.931	1.45e−26	Carbonic anhydrase 12
79401_c1_g1_i8	CAH12	MOUSE	39.286	1.11e−32	Carbonic anhydrase 12
79401_c1_g1_i4	CAH7	MOUSE	37.561	1.12e−42	Carbonic anhydrase 7
80706_c0_g2_i3	CAH14	HUMAN	38.346	6.74e−51	Carbonic anhydrase 14
91001_c3_g5_i1	CAH9	MOUSE	39.216	8.32e−15	Carbonic anhydrase 9
85704_c0_g1_i9	CAH12	HUMAN	37.847	6.08e−58	Carbonic anhydrase 12
72368_c4_g9_i2	CAH12	HUMAN	41.502	5.84e−55	Carbonic anhydrase 12
84685_c0_g1_i6	CAH10	BOVIN	39.827	5.98e−53	Carbonic anhydrase−related protein 10
84685_c0_g1_i1	CAH10	BOVIN	39.932	7.54e−71	Carbonic anhydrase−related protein 10
84685_c0_g1_i5	CAH10	PONAB	36.986	3.66e−11	Carbonic anhydrase−related protein 10
72264_c0_g1_i1	CAH2	CAEEL	42.955	7.96e−76	Putative carbonic anhydrase−like protein 2
67832_c1_g1_i5	CAH6	BOVIN	36.940	3.09e−54	Carbonic anhydrase 6
67832_c1_g1_i4	CAH14	HUMAN	33.987	1.97e−20	Carbonic anhydrase 14
77399_c3_g1_i9	CAH4	RAT	48.780	8.35e−20	Carbonic anhydrase 4
22382_c0_g1_i1	NA	NA	NA	2.10e−05	PF00194.20 Eukaryotic−type carbonic anhydrase
76341_c1_g1_i9	CAHZ	DANRE	37.687	7.07e−51	Carbonic anhydrase
76341_c1_g1_i8	CAH14	MOUSE	34.667	6.01e−07	Carbonic anhydrase 14
76341_c1_g1_i17	CAH6	MOUSE	37.931	3.85e−11	Carbonic anhydrase 6
76341_c1_g1_i1	CAH6	MOUSE	37.931	4.67e−11	Carbonic anhydrase 6
67704_c0_g2_i2	NA	NA	NA	2.20e−09	PF00194.20 Eukaryotic−type carbonic anhydrase
69341_c0_g2_i1	CAH7	MOUSE	41.729	2.62e−55	Carbonic anhydrase 7
69341_c0_g1_i1	CAH7	MOUSE	44.578	1.57e−10	Carbonic anhydrase 7
87572_c0_g4_i1	CAH7	HUMAN	49.655	1.53e−44	Carbonic anhydrase 7

Figure 2. Carbonic Anhydrase (CA) Transcripts. A cladogram depicting the predicted protein sequence similarity between unique transcripts that annotated as carbonic anhydrase and their top BLASTP homolog, the homologs symbol and species abbreviation, percent identity and e-value. Note that transcript 75041_c1_g1_i1 showed homology with a viral cell surface-binding protein that contains a protein domain similar to eukaryotic-type carbonic anhydrase. Additionally, two transcripts (22382_c0_g1_i1 and 67704_c0_g2_i2), did not have a BLASTP homolog but Pfam annoated a protein domain similar to eukaryotic-type carbonic anhydrase (in these instances the e-values is from Pfam).

Unique Acid Sensing Ion Channel (ASIC) Transcripts

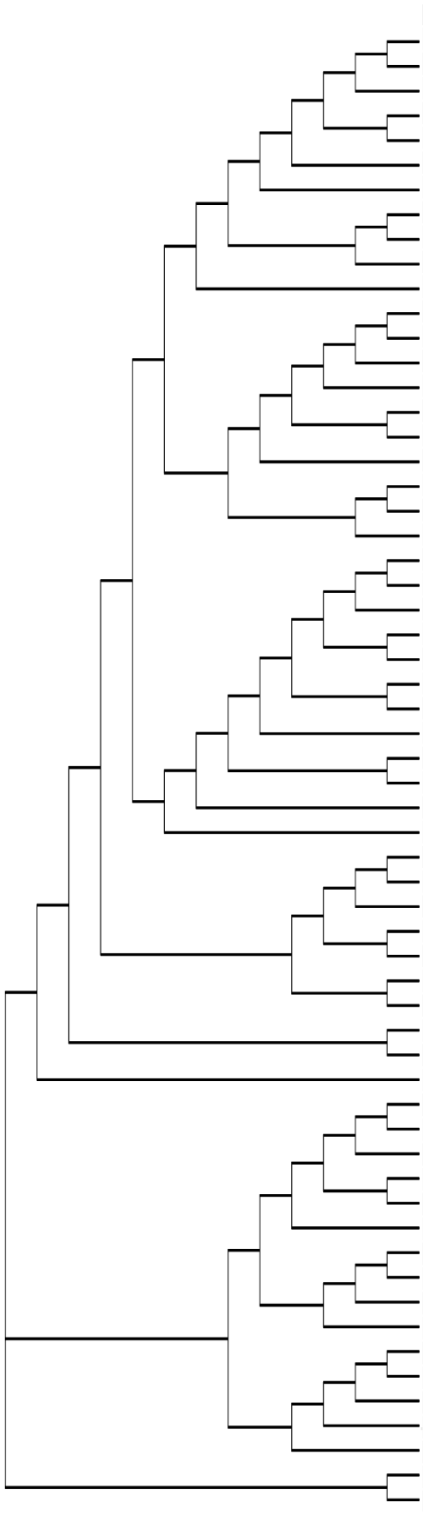

Trinity ID	Symbol	Species	% Idenity	e-Value	Name
86978_c1_g1_i4	ASIC3	HUMAN	28.505	1.11e−09	Acid−sensing ion channel 3
86978_c1_g1_i3	ASIC3	HUMAN	27.320	3.17e−29	Acid−sensing ion channel 3
71711_c0_g1_i1	ASIC5	MOUSE	33.735	7.88e−08	Acid−sensing ion channel 5
77032_c3_g8_i3	ASIC5	MOUSE	34.066	1.96e−10	Acid−sensing ion channel 5
77032_c3_g8_i2	ASIC5	MOUSE	32.967	1.64e−08	Acid−sensing ion channel 5
120732_c0_g1_i1	ASI1A	DANRE	26.207	5.53e−06	Acid−sensing ion channel 1A
77032_c3_g1_i2	ASIC5	RAT	26.329	6.01e−27	Acid−sensing ion channel 5
72917_c0_g1_i3	ASIC5	MOUSE	26.203	5.46e−11	Acid−sensing ion channel 5
72917_c0_g1_i1	ASIC5	MOUSE	26.549	2.21e−12	Acid−sensing ion channel 5
75073_c1_g6_i1	ASIC5	MOUSE	32.955	8.09e−07	Acid−sensing ion channel 5
70739_c0_g3_i1	ASIC5	MOUSE	28.723	7.63e−11	Acid−sensing ion channel 5
57599_c0_g1_i1	ASIC1	RAT	33.094	4.14e−14	Acid−sensing ion channel 1
89038_c1_g1_i19	ASIC2	DANRE	35.821	3.50e−24	Acid−sensing ion channel 2
55481_c2_g1_i1	ASIC1	CHICK	36.111	6.48e−15	Acid−sensing ion channel 1
57306_c0_g2_i4	ASIC3	HUMAN	33.929	3.52e−22	Acid−sensing ion channel 3
89070_c0_g1_i12	ASI4A	DANRE	31.068	2.84e−12	Acid−sensing ion channel 4
89070_c0_g1_i11	ASIC1	HUMAN	28.897	3.01e−29	Acid−sensing ion channel 1
72869_c2_g2_i9	ASIC3	HUMAN	34.959	6.69e−12	Acid−sensing ion channel 3
76439_c3_g5_i5	ASIC2	MOUSE	23.661	1.35e−14	Acid−sensing ion channel 2
76439_c3_g5_i2	ASI4B	DANRE	28.340	4.05e−27	Acid−sensing ion channel 4
76439_c3_g5_i3	ASIC3	HUMAN	31.148	4.88e−20	Acid−sensing ion channel 3
89038_c1_g1_i14	ASI4B	DANRE	42.308	8.16e−11	Acid−sensing ion channel 4
89038_c1_g1_i2	ASI4A	DANRE	42.308	1.77e−10	Acid−sensing ion channel 4
89038_c1_g1_i26	ASI4B	DANRE	50.000	5.73e−11	Acid−sensing ion channel 4
74699_c1_g2_i3	ASI4B	DANRE	47.059	1.52e−08	Acid−sensing ion channel 4
51238_c0_g1_i1	ASI4A	DANRE	42.623	1.36e−08	Acid−sensing ion channel 4
89038_c1_g1_i22	ASI4B	DANRE	31.013	1.31e−12	Acid−sensing ion channel 4
89038_c1_g1_i5	ASI1C	DANRE	33.796	5.70e−32	Acid−sensing ion channel 1C
89038_c1_g1_i1	ASI4B	DANRE	39.744	3.74e−10	Acid−sensing ion channel 4
74699_c2_g6_i3	ASI4A	DANRE	37.624	1.68e−12	Acid−sensing ion channel 4
74699_c2_g6_i1	ASI4A	DANRE	37.624	1.68e−12	Acid−sensing ion channel 4
74132_c0_g2_i1	ASI4B	DANRE	46.667	1.32e−12	Acid−sensing ion channel 4
75685_c3_g3_i7	ASIC1	OPSTA	38.272	1.75e−11	Acid−sensing ion channel 1
87824_c0_g1_i32	ASIC2	RAT	26.522	3.60e−21	Acid−sensing ion channel 2
87824_c0_g1_i19	ASIC2	RAT	26.522	3.60e−21	Acid−sensing ion channel 2
87824_c0_g1_i27	ASIC3	MOUSE	29.464	4.75e−08	Acid−sensing ion channel 3
87824_c0_g1_i8	ASIC2	RAT	28.223	8.84e−29	Acid−sensing ion channel 2
87824_c0_g1_i1	ASIC2	RAT	28.223	8.84e−29	Acid−sensing ion channel 2
75073_c1_g2_i7	ASI1A	DANRE	27.941	1.04e−25	Acid−sensing ion channel 1A
71366_c4_g1_i5	ASIC4	RAT	27.397	4.16e−09	Acid−sensing ion channel 4
75143_c0_g1_i11	ASI4B	DANRE	44.156	1.68e−16	Acid−sensing ion channel 4
75143_c0_g1_i5	ASI4A	DANRE	29.067	4.33e−61	Acid−sensing ion channel 4
76316_c2_g1_i1	ASIC2	RAT	30.216	2.17e−12	Acid−sensing ion channel 2
86978_c1_g4_i4	ASIC1	CHICK	29.450	7.44e−42	Acid−sensing ion channel 1
86978_c1_g4_i3	ASIC3	RAT	31.003	1.49e−40	Acid−sensing ion channel 3
77032_c3_g2_i3	ASIC4	RAT	32.283	1.06e−12	Acid−sensing ion channel 4
81045_c1_g3_i3	ASIC1	CHICK	28.302	6.97e−19	Acid−sensing ion channel 1
81045_c1_g3_i2	ASI1B	DANRE	28.378	8.80e−23	Acid−sensing ion channel 1B
77032_c4_g3_i1	ASIC3	RAT	28.923	4.15e−31	Acid−sensing ion channel 3
72729_c3_g1_i3	ASIC2	RAT	30.841	1.87e−27	Acid−sensing ion channel 2
72729_c3_g1_i2	ASIC2	HUMAN	31.308	1.16e−28	Acid−sensing ion channel 2
72729_c3_g3_i1	ASIC3	HUMAN	30.216	2.21e−32	Acid−sensing ion channel 3
72729_c3_g8_i1	ASIC3	HUMAN	29.054	1.89e−12	Acid−sensing ion channel 3
77032_c4_g2_i6	ASIC1	CHICK	29.570	5.31e−16	Acid−sensing ion channel 1
77032_c4_g2_i3	ASI1B	DANRE	31.250	3.53e−12	Acid−sensing ion channel 1B
77032_c4_g2_i2	ASI1B	DANRE	30.556	2.25e−10	Acid−sensing ion channel 1B
49747_c1_g1_i1	ASIC5	HUMAN	37.143	5.60e−12	Acid−sensing ion channel 5
86978_c1_g1_i5	ASIC3	HUMAN	26.943	4.32e−15	Acid−sensing ion channel 3
138288_c0_g1_i1	ASI1C	DANRE	30.000	1.87e−08	Acid−sensing ion channel 1C
77032_c3_g1_i9	ASIC3	HUMAN	29.197	5.03e−11	Acid−sensing ion channel 3

Figure 3. Acid Sensing Ion Channel (ASIC) Transcripts. A cladogram depicting the predicted protein sequence similarity between unique transcripts that annotated as ASICs and their top BLASTP homolog, the homologs symbol and species abbreviation, percent identity and e-value.

Unique Guanylate Cyclase Transcripts

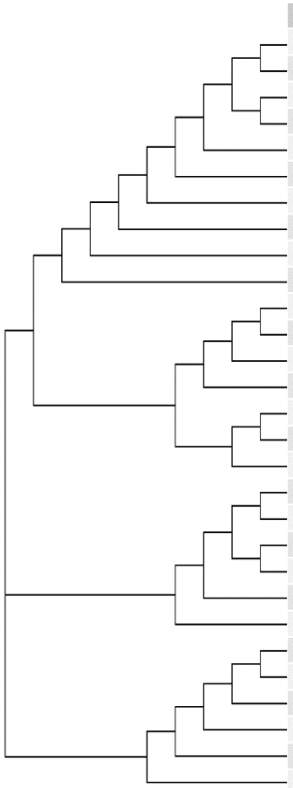

Trinity ID	Symbol	Species	% Idenity	e−Value	Name
81841_c0_g7_i2	GC76C	DROME	63.636	3.18e−63	Receptor−type guanylate cyclase Gyc76C
81841_c0_g7_i1	GC76C	DROME	61.417	2.36e−43	Receptor−type guanylate cyclase Gyc76C
91429_c1_g4_i1	GC76C	DROME	63.684	1.32e−69	Receptor−type guanylate cyclase Gyc76C
48475_c1_g1_i1	GC76C	DROME	62.617	9.83e−41	Receptor−type guanylate cyclase Gyc76C
58278_c0_g1_i3	GUC2G	RAT	56.614	5.86e−67	Guanylate cyclase 2G
81841_c0_g4_i1	GUC2G	RAT	49.169	3.72e−86	Guanylate cyclase 2G
63919_c0_g1_i2	GCYB1	HUMAN	44.944	2.37e−44	Guanylate cyclase soluble subunit beta−1
73631_c5_g2_i1	GUC2G	MOUSE	31.746	2.10e−22	Guanylate cyclase 2G
68349_c0_g2_i1	GUC2G	MOUSE	40.000	1.26e−06	Guanylate cyclase 2G
36899_c0_g1_i1	GC76C	DROME	36.471	4.49e−08	Receptor−type guanylate cyclase Gyc76C
86448_c0_g4_i1	GC76C	DROME	33.673	8.21e−09	Receptor−type guanylate cyclase Gyc76C
124311_c0_g1_i1	GC76C	DROME	31.897	5.58e−11	Receptor−type guanylate cyclase Gyc76C
147425_c0_g1_i1	GCYB1	MOUSE	42.735	2.21e−19	Guanylate cyclase soluble subunit beta−1
18462_c0_g1_i1	GCY8	CAEEL	28.916	7.55e−09	Receptor−type guanylate cyclase gcy−8
5634_c0_g1_i1	GCY17	CAEEL	68.966	7.43e−06	Receptor−type guanylate cyclase gcy−17
85832_c1_g5_i1	GCY28	CAEEL	49.231	1.62e−11	Receptor−type guanylate cyclase gcy−28
46716_c0_g1_i1	GUC2G	RAT	62.338	3.89e−28	Guanylate cyclase 2G
86507_c0_g2_i2	GC76C	DROME	46.844	1.34e−86	Receptor−type guanylate cyclase Gyc76C
86507_c0_g2_i1	GC76C	DROME	46.591	2.33e−21	Receptor−type guanylate cyclase Gyc76C
71524_c3_g1_i4	GC76C	DROME	59.627	0.00e+00	Receptor−type guanylate cyclase Gyc76C
44068_c0_g1_i1	GCY3E	DROME	54.430	3.13e−75	Guanylate cyclase 32E
46379_c0_g1_i1	GCY28	CAEEL	53.175	1.13e−38	Receptor−type guanylate cyclase gcy−28
123201_c0_g1_i1	GUC2G	RAT	24.873	5.29e−06	Guanylate cyclase 2G
80225_c0_g2_i3	GCY28	CAEEL	46.354	6.39e−46	Receptor−type guanylate cyclase gcy−28
80225_c0_g2_i1	GCY28	CAEEL	48.921	4.64e−34	Receptor−type guanylate cyclase gcy−28
87178_c0_g4_i1	GCY28	CAEEL	40.437	1.11e−29	Receptor−type guanylate cyclase gcy−28
79375_c1_g4_i2	GCY28	CAEEL	46.939	4.05e−06	Receptor−type guanylate cyclase gcy−28
79729_c0_g5_i1	GC76C	DROME	29.825	5.29e−08	Receptor−type guanylate cyclase Gyc76C
45452_c0_g1_i1	GCY3E	DROME	42.000	2.58e−19	Guanylate cyclase 32E

Figure 4. Guanylate Cyclase Transcripts. A cladogram depicting the predicted protein sequence similarity between unique transcripts that annotated as Guanylate Cyclase and their top BLASTP homolog, the homologs symbol and species abbreviation, percent identity and e-value.

Unique Otopetrin Transcripts

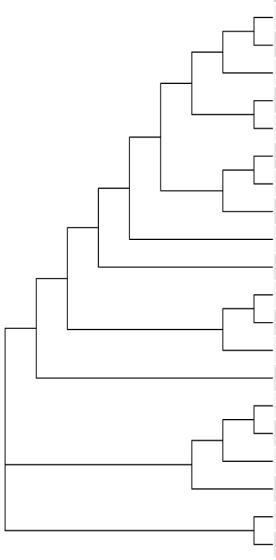

Trinity ID	Symbol	Species	% Idenity	e−Value	Name
85048_c1_g2_i8	OTOP	DROME	25.895	3.71e−44	Proton channel OtopLc {ECO:0000305}
85048_c1_g2_i7	OTOP	DROME	24.623	9.54e−32	Proton channel OtopLc {ECO:0000305}
85048_c1_g2_i2	OTOP	DROME	25.210	6.55e−06	Proton channel OtopLc {ECO:0000305}
76361_c2_g2_i2	OTOP	DROME	31.250	8.60e−09	Proton channel OtopLc {ECO:0000305}
76361_c2_g2_i1	OTOP	DROME	26.396	2.74e−11	Proton channel OtopLc {ECO:0000305}
93135_c4_g1_i6	NA	NA	NA	1.50e−18	PF03189.12 Otopetrin
81113_c0_g1_i2	NA	NA	NA	2.20e−10	PF03189.12 Otopetrin
44104_c0_g1_i1	NA	NA	NA	6.90e−08	PF03189.12 Otopetrin
87198_c1_g2_i4	NA	NA	NA	6.10e−07	PF03189.12 Otopetrin
76361_c2_g1_i6	OTOP	DROME	45.631	1.76e−27	Proton channel OtopLc {ECO:0000305}
85799_c4_g1_i2	NA	NA	NA	1.30e−13	PF03189.12 Otopetrin
81606_c0_g1_i1	NA	NA	NA	4.60e−12	PF03189.12 Otopetrin
75381_c1_g2_i2	NA	NA	NA	3.40e−17	PF03189.12 Otopetrin
84644_c3_g1_i3	OTOP	DROME	26.087	7.19e−08	Proton channel OtopLc {ECO:0000305}
71732_c2_g2_i4	OTOP	DROME	24.713	3.80e−07	Proton channel OtopLc {ECO:0000305}
71732_c2_g2_i2	OTOP	DROME	24.444	6.86e−08	Proton channel OtopLc {ECO:0000305}
85813_c2_g3_i1	NA	NA	NA	2.00e−13	PF03189.12 Otopetrin
72960_c1_g7_i1	NA	NA	NA	2.90e−13	PF03189.12 Otopetrin
69983_c0_g1_i8	OTOP	DROME	29.167	1.00e−05	Proton channel OtopLc {ECO:0000305}
69983_c0_g1_i1	OTOP	DROME	29.167	1.00e−05	Proton channel OtopLc {ECO:0000305}

Figure 5. Otopetrin Transcripts. A cladogram depicting the predicted protein sequence similarity between unique transcripts that annotated as otopetrin and their top BLASTP homolog, the homologs symbol and species abbreviation, percent identity and e-value. Note that several transcripts, did not have a BLASTP homolog but Pfam annotated an otopetrin protein domain (in these instances the e-values is from Pfam).

Unique TRPA1 Transcripts

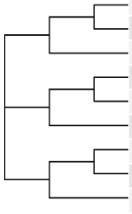

Trinity ID	Symbol	Species	% Idenity	e−Value	Name
36359_c0_g1_i1	TRPA1	DROME	40.625	1.47e−15	Transient receptor potential cation channel subfamily A member 1
53116_c0_g2_i1	TRPA1	HUMAN	44.720	3.16e−39	Transient receptor potential cation channel subfamily A member 1
53116_c0_g1_i1	TRPA1	RAT	40.741	5.96e−25	Transient receptor potential cation channel subfamily A member 1
80430_c2_g1_i3	TRPA1	RAT	35.673	6.56e−19	Transient receptor potential cation channel subfamily A member 1
80430_c2_g1_i2	TRPA1	RAT	35.673	6.56e−19	Transient receptor potential cation channel subfamily A member 1
80430_c2_g1_i9	TRPA1	RAT	35.673	6.56e−19	Transient receptor potential cation channel subfamily A member 1
89448_c3_g1_i2	TRPA1	DROME	42.210	8.65e−76	Transient receptor potential cation channel subfamily A member 1
89448_c3_g1_i1	TRPA1	DROME	42.210	8.65e−76	Transient receptor potential cation channel subfamily A member 1
89448_c3_g1_i5	TRPA1	DROME	51.948	1.66e−40	Transient receptor potential cation channel subfamily A member 1

Figure 6. TRPA Transcripts. A cladogram depicting the predicted protein sequence similarity between unique transcripts that annotated as TRPA1 and their top BLASTP homolog. The homologs symbol and species abbreviation, percent identity and e-value are also listed.

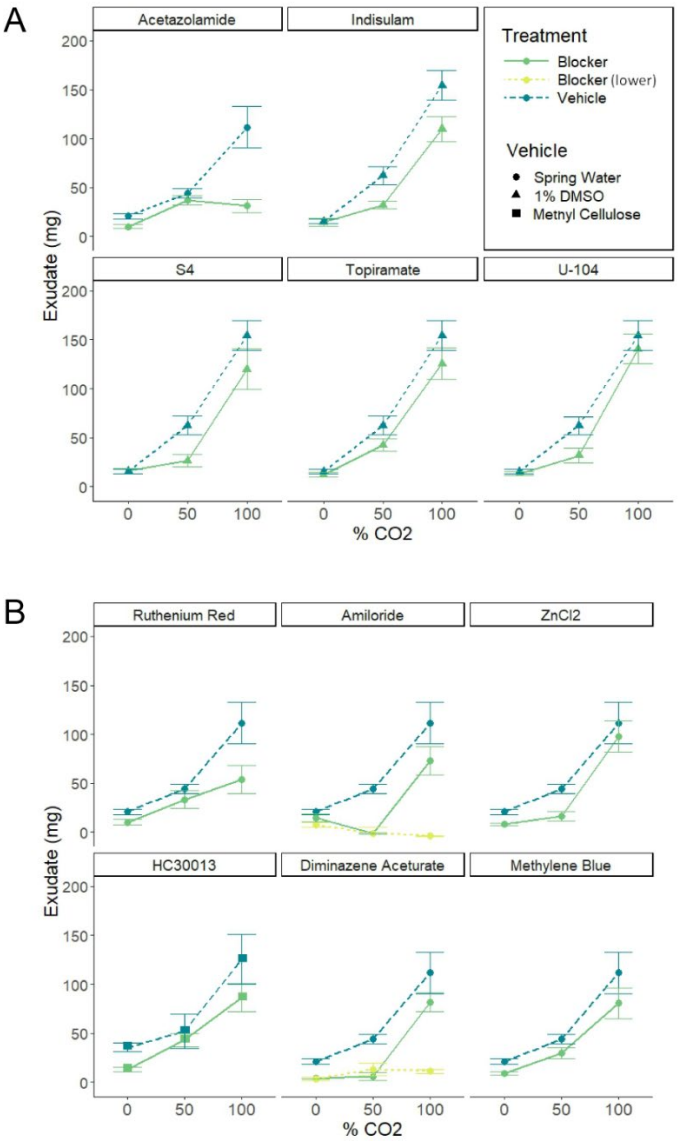

Figure 7. Exudate excretion after treatment with blockers and inhibitors versus treatment with the respective vehicle. A) The carbonic anhydrase inhibitors acetazolamide (general CA inhibitor, p<.001) and indisulam (CA IX/XII inhibitor, p<.01) significantly muted the exudate response by a two-way ANOVA with alpha=.01. S4 (CA IX inhibitor, p<.05) significantly muted the response by a two-way ANOVA with alpha=.05, but a follow-up TukeysHSD showed no significant comparisons. U-104 (CA IX/XII inhibitor, p>.05) and topiramate (CA II/IV inhibitor, p>.05) did not significantly mute the response. B) Receptor blockers amiloride (ENaC blocker, p<.0001), diminazene aceturate (ASIC3 blocker, p<.0001), and ruthenium red (Ca2+ channel blocker, p<.01) significantly muted the exudate response by a two-way ANOVA with alpha=.01. HC030013 (TRPA1 blocker, p<.05), methylene blue (guanylate cyclase inhibitor, p<.05), and ZnCl2 (OTOP1 blocker, p<.05) significantly muted the response by a two-way ANOVA with alpha=.05, but a follow-up TukeysHSD showed no significant comparisons.

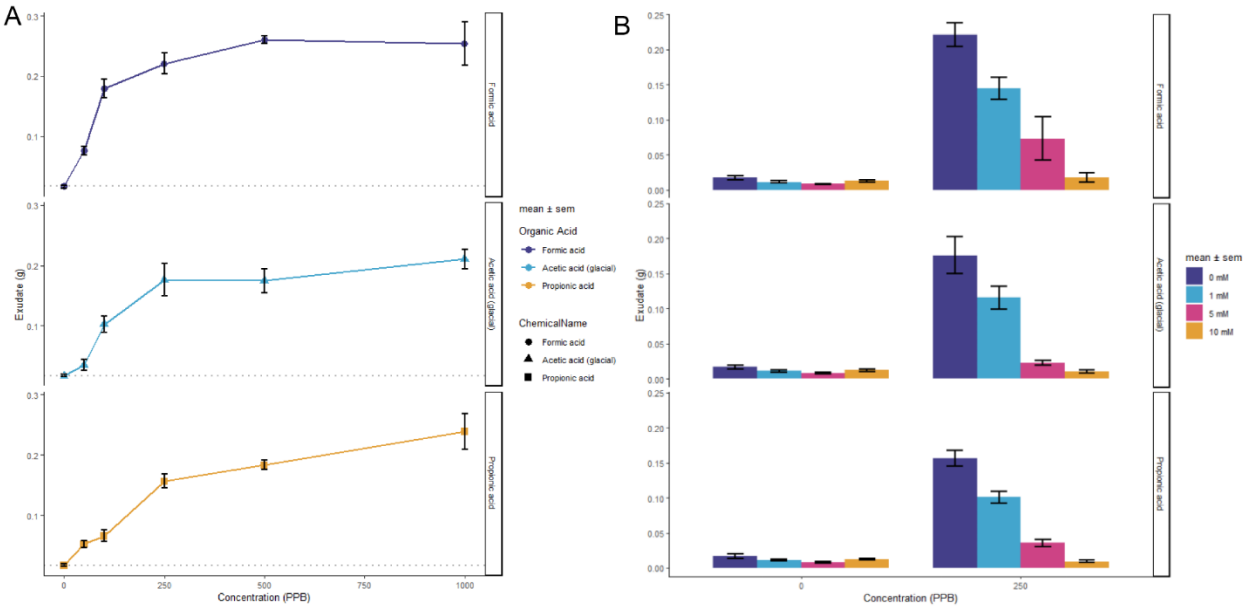

Figure 8. Exudate excretion after exposure to AITC with and without treatment with blockers used in the CO_2 and organic acid experiments. (A) 5mM amiloride (p<.0001), 0.05mM diminazene aceturate (p<.0001), 0.1mM diminazene aceturate (p<001), and HC030013 (p<.0001) significantly muted the response to AITC by a TukeysHSD test, while acetazolamide and indisulam did not (p>.05). Note that amiloride and HC030013 are TRPA1 blockers. (B) Earthworms excrete significantly more exudate in response to increasing concentrations of formic acid, acetic acid, and propionic acid (p<.0001, two-way ANOVA). (C) This response is significantly muted after exposure to amiloride (p<.0001, two-way ANOVA).

Blocker/Inhibitor Name	Concentration	Vehicle	Pharmacology
Acetazolamide	50 mM	H_2O	General carbonic anhydrase inhibitor
Amiloride	1 mM and 5 mM	H_2O	ENaC and ASIC blocker
Diminazene Aceturate	.05 mM and .1 mM	H_2O	ASIC blocker
HC030013	.1 mM	Methyl Cellulose	TRPA1 blocker
Indisulam	.01 mM	1% DMSO in H_2O	Carbonic anhydrase IX and XII inhibitor
Methylene Blue	1 mM	H_2O	Guanylate cyclase inhibitor
Ruthenium Red	.01 mM	H_2O	Calcium channel blocker
S4	.01 mM	1% DMSO in H_2O	Carbonic anhydrase IX inhibitor
Topiramate	.01 mM	1% DMSO in H_2O	Carbonic anhydrase II and IV inhibitor
U-104	.01 mM	1% DMSO in H_2O	Carbonic anhydrase IX and XII inhibitor
$ZnCl_2$	1 mM	H_2O	Otopetrin channel blocker

Table 1. Blockers used in the exudate assay with their concentrations, vehicles, and pharmacological interactions of interest.